

Semantic Misalignment in Vision-Language Models under Perceptual Degradation

Guo Cheng
cheng340@purdue.edu

Abstract

Vision–Language Models (VLMs) are increasingly deployed in autonomous driving and embodied AI systems, where reliable perception is critical for safe semantic reasoning and decision-making. While recent VLMs demonstrate strong performance on multimodal benchmarks, their robustness to realistic perception degradation remains poorly understood. In this work, we systematically study semantic misalignment in VLMs under controlled degradation of upstream visual perception, using semantic segmentation on the Cityscapes dataset as a representative perception module. We introduce perception-realistic corruptions that induce only moderate drops in conventional segmentation metrics, yet observe severe failures in downstream VLM behavior, including hallucinated object mentions, omission of safety-critical entities, and inconsistent safety judgments. To quantify these effects, we propose a set of language-level misalignment metrics that capture hallucination, critical omission, and safety misinterpretation, and analyze their relationship with segmentation quality across multiple contrastive and generative VLMs. Our results reveal a clear disconnect between pixel-level robustness and multimodal semantic reliability, highlighting a critical limitation of current VLM-based systems and motivating the need for evaluation frameworks that explicitly account for perception uncertainty in safety-critical applications.

Key Words: *Vision–Language Models (VLMs), Semantic Segmentation, Perceptual Degradation, Multimodal Misalignment, Hallucination, Autonomous Driving*

1. Introduction

Vision–Language Models (VLMs) have recently achieved remarkable progress in multimodal understanding by jointly reasoning over visual inputs and natural language representations. Many modern models [1–7] demonstrate strong zero-shot and few-shot capabilities across a wide range of vision–language

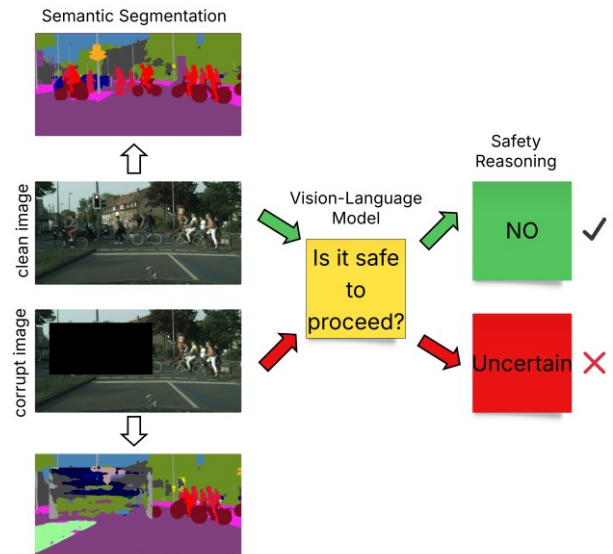


Figure 1: **Conceptual overview of the evaluation pipeline.** Visual inputs are processed by semantic segmentation models under clean and corrupted conditions. While conventional segmentation metrics show limited degradation and preserve plausible semantic structure, the same degraded inputs lead to inconsistent or uncertain Vision–Language Model safety decisions. This reveals a disconnect between perception robustness and multimodal semantic reliability.

benchmarks, leading to growing interest in deploying these models in embodied and safety-critical domains such as autonomous driving and mobile robotics. In such settings, reliable visual perception is a prerequisite for safe and meaningful decision-making. Autonomous systems routinely operate under challenging sensing conditions, where visual inputs are degraded by motion blur, low-light environments, partial occlusions, and sensor noise.

Meanwhile, semantic segmentation plays a foundational role in autonomous driving by providing dense, structured representations of scene semantics and has been extensively studied in prior work [8–10]. Conventional evaluation metrics, such as mean Intersection-over-Union (mIoU) and Pixel Accuracy (PA), are widely used to assess segmentation quality and are often treated as proxies for semantic reliability. Under this paradigm, modest drops in segmentation performance are frequently considered

acceptable, provided that overall scene structure appears visually plausible.

Despite this reliance on perception quality, current VLM-based systems implicitly assume that upstream visual representations remain semantically stable and trustworthy. While the robustness of semantic segmentation under adverse conditions has been studied in isolation, far less is understood about how perception degradation propagates to downstream vision–language reasoning. In particular, it remains unclear whether small changes in conventional segmentation metrics correspond to proportional degradation in multimodal semantic understanding, or whether such degradations can trigger qualitatively different failure modes in VLM outputs.

In this work, we present a systematic empirical study of semantic misalignment in VLMs under controlled degradation of upstream visual perception. Using semantic segmentation on autonomous driving scenes as a representative perception module, we evaluate how perception-realistic corruptions—including motion blur, low-light noise, and partial occlusions—affect downstream language-based scene understanding and safety reasoning. As shown in Fig. 1, we observe that while segmentation outputs often preserve plausible semantic structure and exhibit only moderate degradation in standard metrics, the same corrupted inputs can induce severe failures in VLM behavior, including hallucinated object mentions, omission of safety-critical classes (e.g., pedestrians and traffic signs), and inconsistent or uncertain safety judgments.

To characterize these failures, we introduce a set of interpretable language-level misalignment metrics that explicitly capture hallucination, critical object omission, and safety misinterpretation in VLM outputs. Through experiments on the Cityscapes dataset [11] across multiple contrastive and generative VLMs, we analyze the relationship between segmentation quality and language-level reliability. Our results reveal a weak and inconsistent correlation between conventional segmentation metrics and multimodal semantic reliability, exposing a fundamental disconnect between pixel-level perception robustness and downstream vision–language reasoning.

The main contributions of this work are summarized as:

- **Perception-to-Language Misalignment Analysis.** We present a systematic study of how degradation in semantic segmentation under realistic autonomous driving conditions propagates to semantic misalignment in modern Vision–Language Models.
- **Language-Level Misalignment Metrics.** We propose interpretable metrics to quantify hallucination, critical object omission, and safety misinterpretation in VLM output, capturing failures not reflected by conventional perception metrics.
- **Empirical Decoupling of Perception and Semantic Reliability.** Through controlled

corruption experiments and correlation analysis, we demonstrate that standard segmentation metrics provide limited predictive power for downstream multimodal semantic reliability.

Together, these findings highlight a critical limitation of current VLM-based systems and underscore the need for robustness-aware evaluation frameworks that explicitly account for perception uncertainty in safety-critical multimodal applications.

2. Related Work

2.1. Semantic Segmentation for Autonomous Driving

Semantic segmentation is a core perception task in autonomous driving, enabling dense scene understanding for downstream planning and decision-making. Early deep learning approaches such as Fully Convolutional Networks (FCNs) [12] established pixel-wise prediction as a standard paradigm. Subsequent architectures, including DeepLab and its variants [13,14,29], introduced atrous convolutions and multi-scale context aggregation to improve segmentation accuracy. More recently, transformer-based models such as SegFormer [15] and Mask2Former [16] have further advanced performance by leveraging global context modeling. These models are commonly evaluated on autonomous driving benchmarks [11,17] using metrics including mIoU and per-class IoU. Beyond accuracy, the robustness of semantic segmentation under adverse conditions has received increasing attention. Prior studies examine the effects of motion blur, illumination changes, occlusions, and sensor noise on segmentation [8,9].

While these works provide valuable insights into perception robustness, they primarily focus on segmentation quality in isolation and evaluate robustness solely through conventional pixel-level metrics. How such perception degradation impacts downstream multimodal reasoning remains largely unexplored.

2.2. Vision-Language Models

Vision–Language Models (VLMs) aim to jointly model visual and textual information for multimodal understanding. CLIP [1] introduced large-scale contrastive pretraining on image–text pairs, enabling strong zero-shot transfer across diverse vision tasks. Subsequent models, including BLIP and BLIP-2 [2,22], extend this paradigm by integrating pretrained vision encoders with large language models to support multimodal generation and reasoning. SigLIP [4,5] further improves contrastive alignment through modified training objectives, while instruction-tuned VLMs such as LLaVA [3] and Qwen-VL [6,7] demonstrate impressive performance on visual question answering and multimodal dialogue benchmarks.

Despite their success, existing evaluations of VLMs predominantly rely on curated benchmark datasets and assume reliable visual inputs. As a result, the behavior of VLMs under realistic perception degradation—common in embodied and autonomous systems—remains insufficiently characterized.

2.3. Multimodal Robustness and Hallucination

Recent studies investigated failure modes of VLMs, including object hallucination, spurious correlations, and sensitivity to distribution shifts [18–21]. These works reveal important brittleness in multimodal models, particularly in open-ended generation settings. However, most analyses treat visual inputs as monolithic signals and do not explicitly ground multimodal failures in structured perception outputs such as semantic segmentation.

In parallel, research on uncertainty estimation and safety in autonomous systems emphasizes the importance of reliable perception for downstream reasoning and control [23–28]. While these studies highlight the role of perception uncertainty, the interaction between degraded perception and language-based semantic reasoning has not been systematically examined.

2.4. Summary and Positioning

In summary, prior work has extensively studied (i) semantic segmentation accuracy and robustness, and (ii) vision–language modeling and multimodal reasoning, largely in isolation. What remains missing is a principled analysis of how degradation in structured visual perception—quantified through semantic segmentation—affects semantic reliability in Vision–Language Models. This work bridges these areas by systematically evaluating VLM behavior under controlled perception degradation and introducing language-level misalignment metrics that capture safety-relevant failure modes beyond conventional perception benchmarks.

3. Language-Level Misalignment Metrics

3.1. Motivation

Conventional semantic segmentation metrics such as mean Intersection-over-Union (mIoU) quantify pixel-level agreement between predicted and ground-truth labels. While effective for evaluating visual perception in isolation, these metrics do not capture whether perception errors meaningfully affect downstream multimodal reasoning. In safety-critical autonomous systems, small segmentation errors may lead to qualitatively different failures in semantic interpretation, including hallucinated objects, omission of critical scene elements, or unsafe action recommendations.

To bridge this gap, we introduce **language-level misalignment metrics** that explicitly measure semantic failures in VLM outputs conditioned on degraded visual inputs. These metrics are designed to be interpretable, task-agnostic, and directly relevant to embodied autonomy.

3.2. Problem Setup and Notation

Let

- $x \in X$ denotes a visual input image,
- $\tilde{x} = \mathcal{D}(x)$ denote the degraded image produced by a perception corruption operator \mathcal{D} ,
- $S(\cdot)$ denote a semantic segmentation model,
- $M(\cdot, p)$ denote a Vision–Language Model queried with prompt p .

Let

- y be the ground-truth semantic segmentation for x ,
- $\hat{y} = S(\tilde{x})$ be the predicted segmentation,
- $C_{gt}(x)$ be the set of ground-truth object classes present in the scene,
- $C_{vlm}(\tilde{x})$ be the set of object classes referenced in the VLM’s language output.

3.3. Hallucination Rate (HR)

Hallucination occurs when a VLM references semantic objects that are not present in the visual scene. We define the Hallucination Rate (HR) as:

$$HR = \frac{1}{N} \sum_{i=1}^N \frac{|C_{vlm}(\tilde{x}_i) \setminus C_{gt}(x_i)|}{|C_{vlm}(\tilde{x}_i)| + \epsilon},$$

where N is the number of samples and ϵ prevents division by zero. HR measures the proportion of language outputs that introduce non-existent objects, reflecting overconfidence and semantic fabrication under perception uncertainty.

3.4. Critical Omission Rate (COR)

In autonomous driving, failure to recognize safety-critical objects (e.g., pedestrians, cyclists, traffic signs) can be more severe than hallucinating irrelevant objects. Let $C_{crit} \subset C_{gt}$ denote the set of safety-critical classes. We define the Critical Omission Rate (COR) as:

$$COR = \frac{1}{N} \sum_{i=1}^N I(C_{crit}(x_i) \not\subset C_{vlm}(\tilde{x}_i)),$$

$I(\cdot)$ is the indicator function. COR captures whether VLM fails to mention at least one safety-critical object present in the scene, regardless of overall description quality.

3.5. Safety Misinterpretation Rate (SMR)

Beyond object recognition, autonomous systems require correct semantic interpretation of scene safety. For each image, we query the VLM with a safety-oriented prompt

(e.g., “Is it safe to proceed forward?”) and compare the response against a reference safety label $a_i \in \{\text{safe, unsafe}\}$. We define SMR as:

$$\text{SMR} = \frac{1}{N} \sum_{i=1}^N \mathbb{I}(M(\tilde{x}_i, p_{\text{safe}}) \neq a_i),$$

SMR directly measures the failure of vision–language reasoning to support correct high-level decision-making under degraded perception.

3.6. Correlation with Segmentation Quality

To analyze the relationship between perception quality and multimodal semantic reliability, we compute correlation coefficients between conventional segmentation metrics and the proposed language-level misalignment metrics. Given a segmentation metric Q_i and a misalignment metric L_i , we compute:

$$p(Q, L) = \text{corr}(Q_i, L_i),$$

using both Pearson and Spearman correlations. A key hypothesis is if perception metrics are sufficient proxies for multimodal reliability, strong negative correlations should be observed. Weak or inconsistent correlations indicate a decoupling between segmentation quality and vision–language semantic correctness.

These metrics allow us to characterize failure modes that are invisible to pixel-level evaluation alone. In particular, they expose cases where segmentation degradation is minor by conventional standards yet leads to catastrophic semantic errors in VLM outputs. By explicitly measuring hallucination, omission, and safety misinterpretation, the proposed framework provides a more faithful assessment of multimodal robustness in embodied and autonomous systems.

4. Vision–Language Model Prompt Set

4.1. Prompting Principles

To ensure fair and reproducible evaluation across Vision–Language Models (VLMs), we adopt a fixed, minimal, and task-agnostic prompt set. No prompt tuning or model-specific adaptation is performed. All prompts are:

- Identical across models and datasets
- Zero-shot, without in-context examples
- Free of leading or corrective language
- Designed to probe different levels of semantic understanding

4.2. Prompt Categories

We define three categories of prompts corresponding to increasing semantic complexity:

- **Scene Description Prompt.** It evaluates holistic semantic grounding and serves as the primary

source for extracting referenced object classes and contextual understanding. For example, a prompt as “Describe the scene in this image.” Outputs from this prompt are used to compute HR and COR

- **Object Presence Prompt.** To explicitly probe recognition of safety-critical classes, we define binary object presence prompts. Let $c \in \mathcal{C}_{\text{crit}}$ denote a critical class (e.g., *pedestrian*, *cyclist*, *traffic sign*). For example, a prompt as “Is there a [c] visible in this image? Answer yes or no.” This prompt isolates class-specific recognition errors that may be obscured in free-form descriptions. For evaluation usage, responses are mapped to binary outcomes and contribute to COR and per-class omissions analysis.
- **Safety Interpretation Prompt.** This prompt probes high-level semantic reasoning and the ability of VLMs to integrate perception cues into safety-relevant judgments. For example, a prompt as “Based on this image, is it safe to proceed forward?” Responses are compared against ground-truth safety labels to compute SMR.

4.3. Response Normalization & Prompt Consistency

To reduce variability in language outputs, we apply lightweight normalization:

- Binary responses (*yes/no*, *safe/unsafe*) are mapped to canonical labels
- Free-form responses are parsed using keyword matching for object classes
- Ambiguous or non-committal responses are counted as failures for safety-related prompts

No post-hoc correction or manual filtering is applied. Each degraded image \tilde{x} is evaluated using the same prompt set as its clean counterpart. This ensures that observed changes in language output are attributable solely to perception degradation rather than prompt variation.

We acknowledge that prompt phrasing can influence absolute performance levels. However, our objective is not to maximize VLM accuracy, but to measure relative semantic stability under controlled perception degradation. The use of a fixed, minimal prompt set enables consistent comparison across models, degradation types, and perception pipelines.

5. Methodology and Experimental Setup

This section describes the overall experimental design used to study the relationship between semantic segmentation degradation and vision–language misalignment. We first outline the datasets and perception models used for semantic segmentation, followed by the corruption protocol for controlled perception degradation.

Corruption Type	Severity Level	Implementation Details	Motivation
Motion Blur	s=1	Linear horizontal blur kernel, size 7×7	Mild camera or object motion, common during slow turns or slight ego-motion
	s=2	Linear blur kernel, size 15×15	Moderate ego-vehicle motion or nearby moving objects
	s=3	Linear blur kernel, size 25×25	Severe motion blur during abrupt acceleration, braking, or vibration
Low-Light	s=1	Gamma correction $\gamma = 1.6$ + mild Gaussian noise	Dusk or shaded urban streets
	s=2	Gamma correction $\gamma = 2.2$ + moderate noise	Night-time urban scenes with artificial lighting
	s=3	Gamma correction $\gamma = 3.0$ + stronger noise	Extremely low illumination and sensor noise
Occlusion	s=1	Random rectangular occlusion covering ~8% of image area	Partial occlusion by nearby vehicles or pedestrians
	s=2	Occlusion covering ~15% of image area	Moderate blockage of the field of view
	s=3	Occlusion covering ~25% of image area	Severe occlusion by large foreground objects

Table 1: Image Corruption Types and Severity Levels Used in Evaluation.

We then describe the Vision–Language Models (VLMs), prompting strategy, and evaluation protocol used to quantify semantic misalignment.

5.1. Datasets

For semantic segmentation, Cityscapes [11] provides high-resolution urban street images with fine-grained pixel-level annotations across 19 semantic classes. This dataset serves as canonical benchmark for evaluating semantic segmentation performance under controlled visual degradation.

5.2. Perception Degradation Protocol

To evaluate the robustness of semantic segmentation models under realistic perceptual degradation, we introduce three classes of image corruptions—motion blur, low-light degradation, and partial occlusion—each applied at three increasing severity levels, shown in Table 1.

Motion blur is simulated using a linear convolutional kernel whose size increases with severity, modeling camera shake or rapid ego-motion. Low-light conditions are simulated via gamma correction combined with additive Gaussian noise, capturing illumination loss and sensor noise typical of night-time urban driving. Occlusion is implemented by masking a randomly positioned rectangular region whose area increases with severity, reflecting partial blockage by dynamic objects such as vehicles or pedestrians. These corruptions are applied independently to each test image, resulting in nine degraded variants per image in addition to the original clean input. The corruption parameters are chosen to reflect realistic operational conditions encountered in autonomous driving scenarios while maintaining consistent and reproducible degradation levels across the dataset.

5.3. Semantic Segmentation Evaluation

Semantic segmentation performance is evaluated using standard metrics, including mIoU and per-class IoU. Let

Q_{clean} and Q_{deg} denote segmentation quality on clean and degraded images, respectively. We define the segmentation performance drop as: $\Delta Q = Q_{\text{clean}} - Q_{\text{deg}}$. This quantity captures the magnitude of perception degradation under controlled corruption.

5.4. Vision-Language Models Evaluation

We evaluate multiple Vision–Language Models that represent different classes of multimodal architectures, including both contrastive vision–language representation model and instruction-tuned vision–language model. All VLMs are used in a zero-shot inference setting, without fine-tuning or prompt adaptation. Importantly, all VLMs receive only the raw visual inputs (clean or degraded images). Each model is evaluated on clean images and three corruption types (low-light, motion blur, occlusion) with increasing severity. All generative models are evaluated under a fixed visual token budget to ensure computational stability and fair comparison. Semantic segmentation outputs are used exclusively for analysis and metric computation and are not provided to VLMs.

For each image, we query the VLM using prompts aligned with our proposed metrics:

- **Object grounding:** object presence or top-K object ranking
- **Safety reasoning:** *“Is it safe to proceed forward?”*
- **Hallucination probing:** object predictions not supported by ground truth

Contrastive models (CLIP, SigLIP) use Top-K object selection, while Qwen2-VL generates free-form text parsed into structured outputs.

5.5. Vision-Language Misalignment Analysis

We use a fixed and minimal prompt set designed to probe different levels of semantic understanding, including scene description, object presence recognition, and safety-oriented reasoning, which are defined in Section 4.2. All

Corr.	c1	c2	c3	c4	c5	c6	c7	c8	c9	c10	c11	c12	c13	c14	c15	c16	c17	c18	c19	mIoU
clean	98	84	91	70	59	69	69	74	92	58	93	78	51	93	79	88	81	67	79	77
LL1	97	80	88	63	53	64	58	74	89	60	90	75	47	91	76	81	67	62	78	73
LL2	93	60	75	20	33	46	39	41	73	39	87	60	26	75	33	18	45	10	48	48
LL3	82	33	56	18	11	21	26	14	44	6	70	38	1	41	3	0	3	5	18	26
MB1	96	75	89	57	54	62	64	70	90	56	92	76	55	91	79	86	62	63	76	73
MB2	91	56	83	39	40	40	44	58	85	50	84	60	26	88	69	74	41	33	65	59
MB3	84	39	73	29	28	23	15	33	76	45	67	46	4	76	57	47	19	11	49	43
OCC1	95	78	85	57	39	62	62	69	85	58	91	68	46	74	17	53	69	66	76	66
OCC2	87	71	79	35	25	52	64	64	78	51	83	66	40	61	10	34	62	61	71	58
OCC3	76	61	68	12	12	31	50	53	58	43	69	50	27	56	8	31	0	37	44	41

Table 2: mIoU (%) of all semantic class (c1-c19) in Cityscapes with semantic model of DeepLabV3+. Class of unknow is omitted. (Corr. denotes corruption, LL denotes Low Light, MB denotes Motion Blur, OCC denotes Occlusion, 1/2/3 denotes severity of corruption)

Corr.	DeepLabV3 [13]	SegFormer [15]	Mask2Former [16]
clean	0.77	0.66	0.64
LL1	0.73	0.66	0.59
LL2	0.48	0.67	0.57
LL3	0.26	0.26	0.49
MB1	0.73	0.67	0.58
MB2	0.59	0.60	0.50
MB3	0.43	0.43	0.42
OCC1	0.66	0.66	0.60
OCC2	0.58	0.58	0.50
OCC3	0.41	0.41	0.35

Table 3: mIoU of different models in Cityscapes.

prompts are applied consistently across models, datasets, and degradation levels to ensure fair comparison.

For each image, we obtain VLM outputs on both clean and degraded inputs and compute language-level misalignment metrics, including Hallucination Rate (HR), Critical Omission Rate (COR), and Safety Misinterpretation Rate (SMR), as defined in Section 3. Let L_{clean} and L_{deg} denote a given misalignment metric computed on clean and degraded images, respectively. We define the misalignment increase as $\Delta L = L_{deg} - L_{clean}$. We analyze the relationship between perception degradation (ΔQ) and multimodal semantic misalignment (ΔL) through correlation analysis and stratified evaluation across degradation severity levels.

All experiments are conducted using publicly available implementations. Segmentation and VLM inference are performed independently to avoid cross-contamination between perception and language reasoning. Also, we focus on single-frame semantic segmentation to isolate perception–language coupling effects, deferring temporal analysis to future work.

6. Results

This section presents results evaluating (i) robustness of semantic segmentation under perceptual degradation and (ii) the resulting semantic misalignment in VLMs. We further analyze the relationship between pixel-level perception quality and language-level semantic reliability.

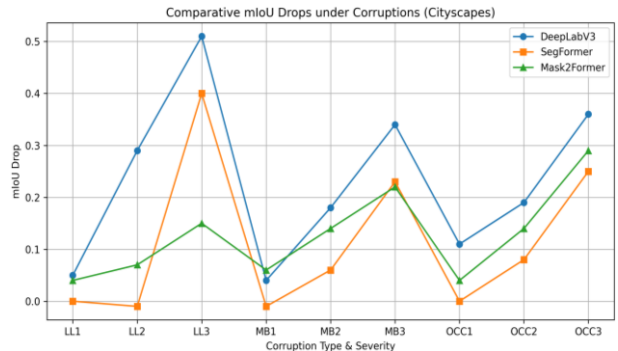


Figure 2: Performance degradation of semantic segmentation on Cityscapes under corruptions.

6.1. Results of Semantic Segmentation Models

We first evaluate the robustness of semantic segmentation models on the Cityscapes dataset under clean and corrupted visual conditions. Table 2 reports class-wise mIoU for DeepLabV3+ under varying corruption types and severities. While overall scene structure is often preserved, safety-critical categories—such as pedestrians, bicycles, and traffic signs—exhibit disproportionately rapid degradation. Under severe low-light and occlusion conditions, several of these classes approach near-zero IoU, even when large structural classes (e.g., road, building) remain visually coherent. This uneven degradation indicates that aggregate metrics such as mIoU can mask failures in safety-relevant perception.

Table 3 summarizes overall mIoU across three representative segmentation models: DeepLabV3+, SegFormer, and Mask2Former. Under clean conditions, DeepLabV3+ achieves the highest mIoU (0.77), followed by SegFormer (0.66) and Mask2Former (0.64). Mild corruptions (LL1, MB1, OCC1) lead to moderate performance drops, whereas severe corruptions result in substantial degradation across all models. Low-light corruption is particularly harmful: under LL3, mIoU drops to 0.26 for both DeepLabV3+ and SegFormer. Motion blur and occlusion induce more gradual degradation, though no model remains reliable at high severity levels.

Corr.	Hallucination Rate	Critical Omission Rate	Safety Misinterpretation Rate
clean	0.17	0.94	0.58
LL1	0.17	0.94	0.6
LL2	0.23	0.94	0.68
LL3	0.22	0.94	0.78
MB1	0.19	0.98	0.52
MB2	0.25	1.0	0.24
MB3	0.23	0.96	0.36
OCC1	0.11	0.8	0.46
OCC2	0.09	0.84	0.42
OCC3	0.12	0.84	0.32

Table 4: Misalignment evaluation of CLIP on Cityscapes dataset under clean and corrupted visual conditions.

Corr.	Hallucination Rate	Critical Omission Rate	Safety Misinterpretation Rate
clean	0.10	0.92	0.8
LL1	0.12	0.9	0.8
LL2	0.14	0.88	0.76
LL3	0.12	0.86	0.74
MB1	0.17	0.92	0.82
MB2	0.13	0.86	0.89
MB3	0.13	0.86	0.88
OCC1	0.08	0.88	0.84
OCC2	0.07	0.84	0.88
OCC3	0.06	0.78	0.88

Table 5: Misalignment evaluation of SigLIP on Cityscapes dataset under clean and corrupted visual conditions.

Fig. 2 visualizes segmentation performance degradation across corruption types and severities. While architectural differences influence robustness trends, all models exhibit pronounced sensitivity under extreme conditions. Importantly, segmentation outputs often remain visually plausible despite significant metric degradation, motivating complementary evaluation beyond pixel-level accuracy when these outputs are used in downstream reasoning.

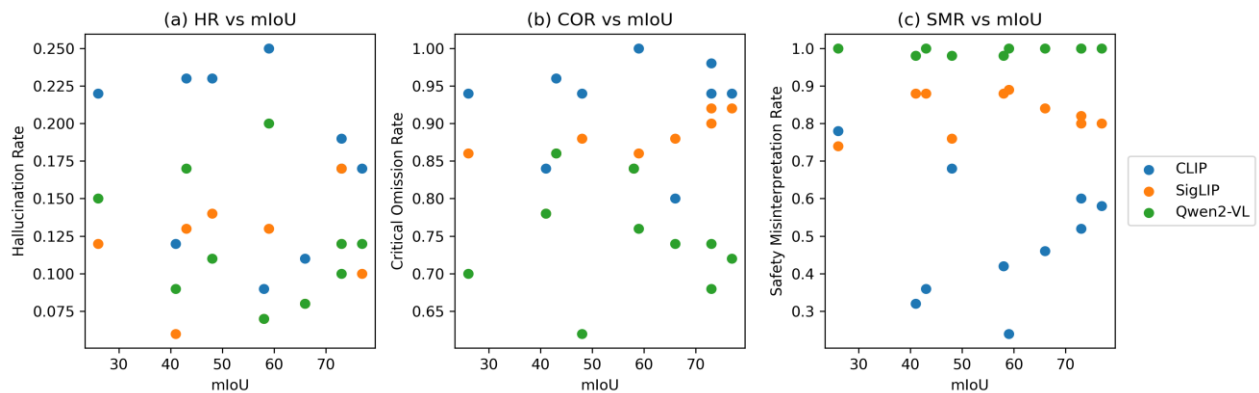


Figure 3: Correlation between segmentation quality and language-level misalignment metrics across 1 clean and 9 corrupted datasets. Notably, several samples exhibit small changes in mIoU but large increases in misalignment metrics, underscoring the inadequacy of aggregate segmentation metrics as predictors of multimodal semantic reliability

Corr.	HR	COR	SMR	safety_parse_success
clean	0.12	0.72	1.0	0.04
LL1	0.1	0.74	1.0	0.02
	0.11	0.62	0.98	0.14
LL3	0.15	0.7	1.0	0.1
MB1	0.12	0.68	1.0	0.1
MB2	0.2	0.76	1.0	0.16
MB3	0.17	0.86	1.0	0.16
OCC1	0.08	0.74	1.0	0.06
OCC2	0.07	0.84	0.98	0.2
OCC3	0.09	0.78	0.98	0.22

Table 6: Misalignment evaluation of Qwen2vl on Cityscapes dataset under clean and corrupted visual conditions, safety_parse_success reflects the fraction of responses yielding a parsable binary decision.

6.2. Results of Visual-Language Models

We next evaluate semantic misalignment in three representative VLMs—CLIP, SigLIP, and Qwen2-VL—using the proposed language-level metrics: Hallucination Rate (HR), Critical Omission Rate (COR), and Safety Misinterpretation Rate (SMR). Results are summarized in Tables 4–6.

For CLIP, HR increases notably under low-light and motion blur, indicating a growing tendency to reference non-existent objects as visual fidelity decreases. COR remains persistently high across conditions, suggesting that safety-critical objects such as pedestrians and traffic signs are frequently omitted from language descriptions despite being present in the scene. SMR exhibits non-monotonic behavior: in some cases, severe corruptions reduce confident but incorrect safety judgments, highlighting unstable and brittle safety reasoning rather than genuine robustness.

SigLIP shows lower hallucination rates overall compared to CLIP, particularly under occlusion, indicating improved resistance to implausible object generation. However, COR remains high across all corruption levels,

and SMR consistently exceeds 0.7, demonstrating that reduced hallucination does not translate to reliable safety interpretation. This decoupling suggests that object-level

grounding alone is insufficient for robust high-level reasoning.

Qwen2-VL exhibits comparatively lower HR and COR under several corruption settings, but SMR approaches

Input Image	Semantic Segmentation			VLM prompts		
	DeepLabV3+ [13]	SegFormer [15]	Mask2Former [16]	Scene Description	Object Presence	Safety Interpret.
				The image shows an urban intersection where multiple cyclists and pedestrians are crossing the road in front of the ego vehicle. The traffic light ahead is red, and the ego vehicle is stopped while vulnerable road users move through the crosswalk. Buildings, trees, and traffic infrastructure surround the intersection, indicating a typical city environment.	car: false, truck: false, bus: false, motorcycle: false, bicycle: true, pedestrian: true, traffic light: true, traffic sign: true	decision: NO, reason: Pedestrians and cyclists are actively crossing the intersection in front of the vehicle.
				The image depicts an urban intersection where several cyclists and pedestrians are crossing the road in front of the ego vehicle. The traffic light is red, and the ego vehicle remains stopped while vulnerable road users move across the crosswalk. Residential buildings, trees, and traffic infrastructure are visible around the intersection.	car: false, truck: false, bus: false, motorcycle: false, bicycle: true, pedestrian: true, traffic light: true, traffic sign: true	decision: NO, reason: Cyclists and pedestrians are currently crossing the road in front of the ego vehicle.
				The image shows an urban intersection at low-light conditions where multiple cyclists and pedestrians are crossing the road in front of the ego vehicle. A red traffic light is clearly visible, indicating that the ego vehicle is stopped while vulnerable road users proceed through the crosswalk. Residential buildings, trees, and traffic infrastructure surround the intersection.	car: false, truck: false, bus: false, motorcycle: false, bicycle: true, pedestrian: true, traffic light: true, traffic sign: true	decision: NO, reason: Multiple cyclists and pedestrians are crossing directly in front of the ego vehicle under a red light.
				The image shows a darkened urban intersection under very low-light conditions, with visibility significantly reduced. Several cyclists and pedestrians are crossing the road at a marked crosswalk while a red traffic light is visible ahead. Buildings, trees, and roadside infrastructure are faintly discernible in the background.	car: false, truck: false, bus: false, motorcycle: false, bicycle: true, pedestrian: true, traffic light: true, traffic sign: true	decision: NO, reason: Multiple cyclists and pedestrians are crossing in front of the vehicle under low visibility with a red traffic light.
				The image depicts an urban intersection where several cyclists and pedestrians are crossing in front of the ego vehicle at a marked crosswalk. A red traffic light is visible, indicating the ego vehicle is required to stop while vulnerable road users proceed. Mild motion blur slightly affects clarity but the scene remains largely interpretable.	car: false, truck: false, bus: false, motorcycle: false, bicycle: true, pedestrian: true, traffic light: true, traffic sign: true	decision: NO, reason: Cyclists and pedestrians are actively crossing the intersection while the ego vehicle is red.
				The image shows an urban intersection where multiple cyclists and pedestrians are crossing the road in front of the ego vehicle, but the scene is heavily affected by motion blur. Despite the reduced sharpness, the red traffic light and the general movement of vulnerable road users across the crosswalk are still discernible. The ego vehicle appears to be stopped while cross traffic proceeds.	car: false, truck: false, bus: false, motorcycle: false, bicycle: true, pedestrian: true, traffic light: true, traffic sign: true	decision: NO, reason: Pedestrians and cyclists are crossing ahead under a red traffic light despite reduced visibility from motion blur.
				The image depicts an urban intersection where strong motion blur significantly reduces visual clarity. Several cyclists and pedestrians are crossing the road at a crosswalk while a red traffic light is visible ahead. Despite the blur, the presence of multiple vulnerable road users in front of the ego vehicle is still apparent.	car: false, truck: false, bus: false, motorcycle: false, bicycle: true, pedestrian: true, traffic light: true, traffic sign: true	decision: NO, reason: Cyclists and pedestrians are crossing at a red light, motion blur further reduces confidence in safe forward.
				The image depicts an urban intersection where multiple cyclists and pedestrians are crossing the road at a marked crosswalk in front of the ego vehicle. A red traffic light is clearly visible, indicating the vehicle must stop, while a large black occlusion blocks the lower-right portion of the scene. Despite the occlusion, many vulnerable road users are still visible directly ahead.	car: false, truck: false, bus: false, motorcycle: false, bicycle: true, pedestrian: true, traffic light: true, traffic sign: true	decision: NO, reason: Cyclists and pedestrians are crossing in front of the vehicle while the traffic light is red.
				The image shows an urban intersection where multiple cyclists and pedestrians are crossing the road at a marked crosswalk. A red traffic light is visible for the ego vehicle, while a large occluding black region blocks part of the right-hand side of the scene. Despite the occlusion, several vulnerable road users are clearly present in front of the vehicle.	car: false, truck: false, bus: false, motorcycle: false, bicycle: true, pedestrian: true, traffic light: true, traffic sign: true	decision: NO, reason: Pedestrians and cyclists are crossing at a red light, and the occluded region limits visibility of the full scene.
				The image depicts an urban intersection where a large occlusion blocks the central field of view, partially obscuring the roadway and some traffic participants. On the visible right side, several cyclists and pedestrians are crossing the street at a marked crosswalk. The scene appears to be a residential area with traffic infrastructure and signage present.	car: false, truck: false, bus: false, motorcycle: false, bicycle: true, pedestrian: true, traffic light: true, traffic sign: true	decision: UNCERTAIN, reason: A large occlusion blocks much of the scene, limiting visibility of potential hazards.

Figure 4: Semantic segmentation results of different models on Cityscapes under various corruptions, together with a proprietary GPT-family model-generated scene understanding and safety reasoning (from top to bottom: clean, I11-3, mb1-3, occ1-3). Under severe occlusion, VLM safety decisions may become unreliable even when segmentation outputs remain visually plausible.

saturation across nearly all conditions. Further analysis reveals that this behavior is largely driven by frequent generation of ambiguous or uncertain safety responses, uncertainty may reduce confidently incorrect decisions, it nonetheless represents a failure mode for autonomous systems that require actionable safety judgments.

Overall, these results demonstrate that **perception degradation induces qualitatively different failure modes in VLMs**, including hallucination, omission, and unstable safety reasoning. Crucially, these failures are not reliably predicted by conventional segmentation metrics, underscoring a fundamental disconnect between pixel-level perception quality and multimodal semantic reliability.

6.3. Correlation Between Perception Quality and Semantic Misalignment

To analyze the relationship between perception robustness and multimodal semantic reliability, we examine correlations between segmentation quality (mIoU) and language-level misalignment metrics. Fig. 3 illustrates these relationships across clean and corrupt conditions. Notably, several points in Fig. 3 exhibit minimal changes in mIoU while incurring large increases in HR, COR, or SMR. This behavior does not indicate inconsistency, but rather highlights the insensitivity of aggregate segmentation metrics to localized, safety-critical perception errors that disproportionately affect vision-language reasoning.

Critical Omission Rate (COR) shows a moderate negative correlation with mIoU, indicating that reduced pixel-level perception quality increases the likelihood of missing safety-critical objects in VLM outputs. In contrast, Hallucination Rate (HR) exhibits weak and inconsistent correlation with segmentation quality, suggesting that hallucination is not directly governed by pixel-level accuracy. Most notably, Safety Misinterpretation Rate (SMR) demonstrates minimal correlation with mIoU across all evaluated models. For Qwen2-VL in particular, safety failures persist even when segmentation quality remains relatively high. These results reveal a clear decoupling between conventional segmentation metrics and higher-level semantic and safety reliability. While segmentation outputs may remain visually coherent under degradation, downstream vision-language reasoning can fail catastrophically.

Fig. 4 provides qualitative examples illustrating this disconnect. Under severe occlusion, segmentation outputs remain plausible, yet VLM-generated scene interpretations and safety judgments become inconsistent or unreliable. Similar behavior is observed when evaluating a proprietary GPT-family model, reinforcing that this failure mode is not limited to a specific architecture.

7. Conclusion

This paper presents a systematic study of semantic misalignment in Vision-Language Models under realistic degradation of upstream visual perception. Using semantic segmentation on the Cityscapes dataset as a representative perception module, we demonstrate that modest degradation in conventional segmentation metrics can trigger severe failures in downstream multimodal reasoning. These failures manifest as hallucinated object mentions, omission of safety-critical entities, and incorrect or uncertain safety judgments, even when segmentation outputs remain visually plausible.

To capture these phenomena, we introduce language-level misalignment metrics that explicitly quantify hallucination, critical omission, and safety misinterpretation. Through extensive experiments across contrastive and generative VLMs, we show that conventional perception metrics such as mIoU exhibit weak and inconsistent correlation with multimodal semantic reliability. In particular, safety reasoning failures persist even under relatively high segmentation quality, revealing a fundamental disconnect between pixel-level robustness and semantic reliability.

Our findings highlight a critical limitation of current VLM-based systems for autonomous and embodied applications. Evaluating perception and language components in isolation is insufficient to guarantee reliable multimodal behavior under real-world conditions. Future work should explore tighter integration of perception uncertainty into vision-language reasoning, robustness-aware training objectives, and evaluation frameworks that directly reflect safety-relevant semantic failures. We hope this work motivates a shift toward holistic, uncertainty-aware evaluation of multimodal systems in safety-critical domains.

8. Future Work

While this work focuses on single-frame semantic segmentation to isolate the relationship between perception degradation and vision-language misalignment, an important direction for future research is extending the proposed evaluation framework to sequential semantic segmentation and video-based perception. Temporal aggregation and consistency mechanisms may stabilize pixel-level predictions under dynamic conditions, but it remains unclear whether such temporal robustness translates to improved semantic reliability in downstream vision-language reasoning. Applying the proposed misalignment metrics to temporally coherent perception pipelines would enable systematic study of error accumulation, temporal hallucination, and safety drift over time. We leave this investigation to future work.

References

- [1] A. Radford, J. Kim, C. Hallacy, A. Ramesh, G. Goh, S. Agarwal, G. Sastry, A. Askell, P. Mishkin, J. Clark, et al. Learning transferable visual models from natural language supervision. *International Conference on Machine Learning (ICML)*, 2021.
- [2] J. Li, D. Li, S. Savarese, S. Hoi. BLIP-2: Bootstrapping Language-Image Pre-training with Frozen Image Encoders and Large Language Models. *International Conference on Machine Learning (ICML)*, 2023.
- [3] H. Liu, C. Li, Q. Wu, Y. Lee. Visual Instruction Tuning. *NeurIPS*, 2023.
- [4] X. Zhai, B. Mastafa, A. Kolesnikov, L. Beyer. Sigmoid Loss for Language Image Pre-Training. *ICCV*, 2023.
- [5] M. Tschannen, A. Gritsenko, X. Wang, M. Naeem, I. Alabdulmohsin, N. Parthasarathy, T. Evans, L. Beyer, Y. Xia, B. Mustafa, O. Hénaff, J. Harmsen, A. Steiner, X. Zhai. SigLIP 2: Multilingual Vision-Language Encoders with Improved Semantic Understanding, Localization, and Dense Features. *arXiv preprint arXiv:2502.1478*, 2025.
- [6] Pe. Wang, S. Bai, S. Tan, S. Wang, Z. Fan, J. Bai, K. Chen and X. Liu, J. Wang, W. Ge, Y. Fan, K. D. M. Du, X. Ren, R. Men, D. Liu, C. Zhou, J. Zhou, J. Lin. Qwen2-VL: Enhancing Vision-Language Model’s Perception of the World at Any Resolution. *arXiv preprint arXiv:2409.12191*, 2024.
- [7] Bai et al. Qwen2.5-VL Technical Report, *arXiv:2502.13923*, 2025.
- [8] G. Cheng, J. Zheng, M. Kilicarslan, Semantic Segmentation of Road Profiles for Efficient Sensing in Autonomous Driving, *IEEE Intelligent Vehicles Sympo.*, 564-569, 2019.
- [9] G. Cheng, J. Zheng, Semantic Segmentation for Pedestrian Detection from Motion in Temporal Domain, *25th Inter. Conf. Pattern Recognition (ICPR)*, 2020.
- [10] G.Cheng, J. Zheng. Sequential Semantic Segmentation of Road Profiles for Path and Speed Planning. *IEEE Transactions on Intelligent Transportation Systems (T-ITS)*, 2022.
- [11] M. Cordts, M. Omran, S. Ramos, T. Rehfeld, M. Enzweiler, R. Benenson, U. Franke, S Roth, B. Schiele. The Cityscapes Dataset for Semantic Urban Scene Understanding. *CVPR*, 2016.
- [12] J. Long, E. Shelhamer, T. Darrel, Fully convolutional networks for semantic segmentation, *CVPR*, pp. 3431- 3440, 2015.
- [13] L. Chen, G. Papandreou, I. Kokkinos, K. Murphy, A. Yuille. Deeplab: Semantic Image Segmentation with Deep Convolutional Nets, Atrous Convolution, and Fully Connected CRFs. *TPAMI*, 2017.
- [14] B. Cheng, M. Collins, Y. Zhu, T. Liu, T. Huang, H. Adam, L. Chen. Panoptic-DeepLab: A Simple, Strong, and Fast Baseline for Bottom-Up Panoptic Segmentation. *CVPR*, 2020.
- [15] E. Xie, W. Wang, Z. Yu, A. Anandkumar, J. Alvarez, P. Luo. SegFormer: Simple and Efficient Design for Semantic Segmentation with Transformers. *NeurIPS*, 2021.
- [16] B. Cheng, I. Misra, A. Schwing, A. Kirillov, R. Girdhar. Masked-Attention Mask Transformer for Universal Image Segmentation. *CVPR*, 2022.
- [17] F. Yu, H. Chen, X. Wang, W.Xian, Y. Chen, F. Liu, V. Madhavan, T. Darrell. BDD100K: A Diverse Driving Dataset for Heterogeneous Multitask Learning. *CVPR*, 2020.
- [18] D. Hendrycks, T. Dietterich. Benchmarking Neural Network Robustness to Common Corruptions and Perturbations. *ICML*, 2019.
- [19] C. Kamann, C. Rothe. Benchmarking the Robustness of Semantic Segmentation Models. *CVPR*, 2020.
- [20] D. Nilsson, C. Sminchisescu. Semantic Video Segmentation by Gated Recurrent Flow Propagation. *CVPR*, 2018.
- [21] S. Jain, X. Wang, J. Gonzalez. Accel: A Corrective Fusion Network for Efficient Semantic Segmentation on Video. *CVPR*, 2019.
- [22] J. Li, D. Li, C. Xiong, S. Hoi. BLIP: Bootstrapping Language-Image Pre-training for Unified Vision-Language Understanding and Generation. *International Conference on Machine Learning (ICML)*, 2022.
- [23] A. Rohrbach, L. Hendricks, K. Burns, T. Darrell, K. Saenko. Object Hallucination in Image Captioning. *EMNLP*, 2018.
- [24] S. Leng, H. Zhang, G. Chen, X. Li, S. Lu, C. Miao, L. Bing. Mitigating Object Hallucinations in Large Vision-Language Models through Visual Contrastive Decoding. *CVPR*, 2024.
- [25] J. Qiu, Y. Zhu, X. Shi, F. Wenzel, Z. Tang, D. Zhao, B. Li, M. Li. Benchmarking Robustness of Multimodal Image-Text Models under Distribution Shift. *Journal of Data-centric Machine Learning Research (DMLR)*, 2024.
- [26] C. Schlarmann, N. Singh, C. Francesco, et al. Robust clip: Unsupervised adversarial fine-tuning of vision embeddings for robust large vision-language models. *ICML*, 2024.
- [27] A. Kendal, Y. Gal. What Uncertainties Do We Need in Bayesian Deep Learning for Computer Vision? *NeurIPS*, 2017.
- [28] R. Michelmoro, M. Kwiatkowska, Y. Gal. Evaluating Uncertainty Quantification in End-to-End Autonomous Driving Control. *arXiv preprint arXiv:1811.06817*, 2018.
- [29] L. Chen, Y. Zhu, G. Papandreou, F. Schroff, H. Adam. Encoder-Decoder with Atrous Separable Convolution for Semantic Image Segmentation. *ECCV*, 2018.
- [30] OpenAI, GPT-4 Technical Report. *arXiv preprint arXiv:2303.08774*, 2024.